RSC Advances

ROYAL SOCIETY OF CHEMISTRY

www.rsc.org/advances

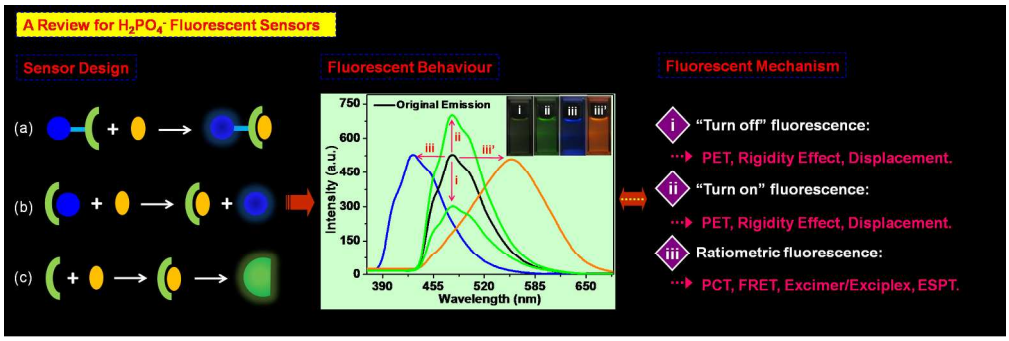

419x139mm (150 x 150 DPI)

Cite this: DOI: 10.1039/c0xx00000x

www.rsc.org/xxxxxx

ARTICLE TYPE

Recent advances in $H_2PO_4^-$ fluorescent sensors

Dawei Zhang,[a,b] James Robert Cochrane,[b] Alexandre Martinez*[b] and Guohua Gao*[a]

Received (in XXX, XXX) Xth XXXXXXXXX 20XX, Accepted Xth XXXXXXXXX 20XX
DOI: 10.1039/b000000x

Dihydrogen phosphate ($H_2PO_4^-$) plays an essential role in a number of chemical and biological processes. The sensitive and selective detection of $H_2PO_4^-$ is of great interest to many scientific fields, ranging from supramolecular chemistry to life sciences. For the detection of $H_2PO_4^-$, fluorescent methods have plenty of distinct advantages, for example they are simplistic and allow low levels of determination. Therefore, this review will focus on the current progress in the development of $H_2PO_4^-$ fluorescent sensors based on organic scaffolds, for sensing in both organic and aqueous solutions. Three main types of fluorescent probes will be categorized in this review: (i) intensity-based "turn-off" fluorescent sensors; (ii) intensity-based "turn-on" fluorescent sensors; and (iii) ratiometric fluorescent sensors that involve a ratio of two emission outputs. This review should provide a comprehensive description of this research area to date and be instructive for the design and synthesis of new fluorescent sensors for $H_2PO_4^-$. In addition, the principles and mechanisms employed in the design of $H_2PO_4^-$ sensors will be thoroughly described.

1. Introduction

Inorganic phosphate species are biologically relevant anions that have essential roles in genetic information storage, gene regulation, energy transduction, signalling processing and muscle contraction.[1,2] Phosphate is also a key constituent of two important biopolymers, DNA and RNA as well as many chemotherapeutic and antiviral drugs.[3,4] On the other hand, the over-use of inorganic phosphate in agriculture can lead to excessive algal growth, followed by decomposition and depletion of dissolved oxygen, and ultimately, the eutrophication of aquatic ecosystems.[5] Dihydrogen phosphate ($H_2PO_4^-$) is the predominant equilibrium species of inorganic phosphate at physiological pH. Therefore, $H_2PO_4^-$ is an important target anion, and methods for its detection have received increasing attention of late.[6-10]

The development of sensors for the recognition and detection of anions is of great importance in the field of modern supramolecular chemistry.[11-15] In this field fluorescent sensors bear inherent advantages, these include their high sensitivity, simple manipulation and facile visualization. All of these are essential properties for bio-imaging and thus the design of fluorescence-based probes for the detection of $H_2PO_4^-$ is an important area of research.[16-26] Artificial fluorescent anion sensors belong to one of the following three design approaches (Scheme 1, A): (a) The "binding site-signalling unit", the interaction of the binding site(s) with anions, causes the change of the electronic properties of the signalling unit. Fluorescent mechanisms that commonly involved in this approach include photo-induced electron transfer (PET), the rigidity effect, fluorescence resonance energy transfer (FRET), excimer/exciplex formation/extinction, photo-induced charge transfer (PCT), and less frequently, excited-state proton transfer (ESPT). (b) The "displacement" protocol, in which the introduction of anions to the coordinated metal complex revives the non-coordinated spectroscopic properties of the indicator. (c) The reaction-based

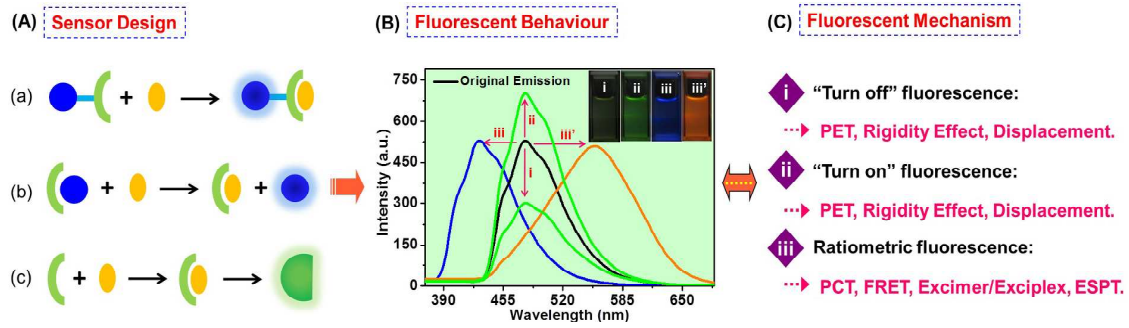

Scheme 1 (A) The approaches for designing fluorescent sensors: (a) "binding site-signalling unit" approach; (b) displacement approach; (c) reaction-based chemodosisensor. (B) The possible fluorescent behaviours after anion binding: (i) "turn off" fluorescence; (ii) "turn on" fluorescence; (iii) ratiometric fluorescence. (C) The possible fluorescent mechanisms involved in the corresponding fluorescent behaviours.

strategy which occurs between the target anions and the "chemodosisensor". It is worth mentioning that until now, all the $H_2PO_4^-$ fluorescent sensors have fallen into the first two categories, and there has been no reported chemodosisensor for $H_2PO_4^-$ sensing.

The fluorescent phenomena observed after $H_2PO_4^-$ binding also follows three main patterns of behaviour (Scheme 1, B): fluorescence quenching, enhancement at the original wavelength, and ratiometric sensing that involves a comparison of intensities at two different emission outputs. Generally the fluorescent behaviour observed depends on the initial design of the sensor (Scheme 1, C). (i) For sensors adopting the "binding site-signalling unit" approach, the mechanisms of PET and rigidity effect may quench or enhance the fluorescence of the probe after anion binding, while the FRET, excimer/exciplex formation/extinction, PCT, and ESPT can cause the bathochromic/hypochromatic-shift of the emission resulting in a ratiometric sensing behaviour. (ii) For sensors utilizing the "displacement" protocol, the fluorescent change of the coordinated complex induced by $H_2PO_4^-$ is usually consistent with the initial non-coordinated indicator.

In the last decade, there have been reviews dealing with the subject of phosphate detection,[8,9] bio-phosphate recognition,[6,7,10] and pyrophosphate fluorescent sensing,[27] however to the best of our knowledge, there is no comprehensive review which thoroughly, systematically and timely describes fluorescent sensing of $H_2PO_4^-$. As $H_2PO_4^-$ is in equilibrium with two other basic anions HPO_4^{2-} and PO_4^{3-} at physiological pH,[8] the selective sensing of $H_2PO_4^-$ is especially important as well as challenging. For this reason in this review, we only highlight the detection of $H_2PO_4^-$. In terms of the fluorescent behaviour observed upon $H_2PO_4^-$ binding, we have classified the fluorescent probes based on their modes of action. Fluorescent probes exhibiting "turn-off" detection are covered in Section 2, "turn-on" in Section 3 and ratiometric sensing in Section 4. We subdivide the content of each section into the sensing mechanisms involved. This classification should promote a better understanding of the anion-induced fluorescent behaviour and will be instructive for the design of more selective sensors with the desired fluorescent properties. It should be made clear that in some cases, the mechanism of fluorescence is inferred by the authors and are not demonstrated absolutely. In some instances, two or more possible mechanisms might simultaneously exist in the sensing process, and in these situation, we place the sensor into the category where it can be best explained. It should also be highlighted that the selective recognition of $H_2PO_4^-$ over other common anions is one of the most important issues to be addressed, thus the selectivity of each sensor has been evaluated.

2. Intensity-based "turn-off" fluorescent sensors for $H_2PO_4^-$

In this section, fluorescent sensors that provide "turn-off" fluorescence detection of $H_2PO_4^-$ will be described. Fluorescence quenching by $H_2PO_4^-$ is a commonly encountered phenomenon which provides a facile approach for monitoring this important anion. PET is one of the most extensively adopted mechanisms for fluorescence quenching (Section 2.1 and Scheme 2). Upon the binding of $H_2PO_4^-$, the PET process of the sensor is initiated or promoted (Scheme 2a), causing a corresponding decrease in the fluorescence of the sensor. The other methods used in fluorescence detection, such as "displacement" and ligand-to-metal charge transfer are discussed in Sections 2.2 and 2.3. For convenient comparison, the spectroscopic and analytical parameters of each "turn off" fluorescent sensor for $H_2PO_4^-$ have been summarized in Table 1.

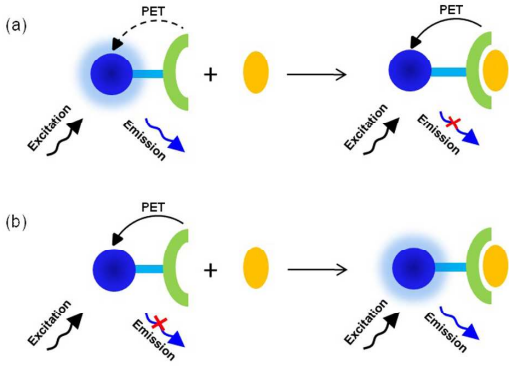

Scheme 2 Diagrams for (a) the initiation or promotion of PET and (b) the inhibition of PET after anion binding.

2.1 Initiation or promotion of PET

The fluorescent sensor (**1**) reported by Kim et al.[28] (Fig. 1) bearing two imidazolium groups at the 1, 8-position of anthracene showed significant fluorescence quenching in CH_3CN upon addition of $H_2PO_4^-$. This was due to the formation of $(C\text{-}H)^+\ldots X^-$ hydrogen bonds. The binding constant of **1** with $H_2PO_4^-$ was found to be relatively large (1.3×10^6 M^{-1}), however strong competition by F^- for $H_2PO_4^-$ binding was observed. To circumvent this, their group subsequently designed the rigid fluorescent sensor **2**. Based on the scaffold of **1** two anthracene units were directly connected by the two imidazolium moieties forming a cyclic receptor.[29] Significant fluorescence quenching of sensor **2** occurred after addition of $H_2PO_4^-$ in CH_3CN/DMSO (9 : 1, v/v) due to the PET process. More importantly, competitive binding studies demonstrated that there is no interference of the binding of $H_2PO_4^-$ even when in the presence of 1.5 equiv. of F^-. The binding constant of sensor **2** with $H_2PO_4^-$ was also found to be larger than that of sensor **1** ($>1.3\times10^6$ M^{-1}).

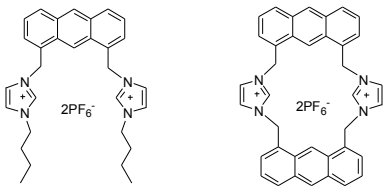

1 2

Fig. 1 Structures of sensors **1** and **2**.

Bearing the concept of the PET process between imidazolium binding sites and the excited state of anthracene in mind, Jadhav et al.[30] developed an anthracene-imidazolium-based macrocyclic sensor (**3**) (Fig. 2). In this sensor the two pendant imidazolium arms are connected by attachment to a molecule of cholestane.[31] The sensor **3** exhibited 95% fluorescence quenching after addition of 10 equiv. of $H_2PO_4^-$ in CH_3CN with a binding constant of 1.6×10^5 M^{-1}, while only 20-40% decrease in intensity

Table 1 Spectroscopic and analytical parameters of the "turn off" fluorescent sensors for $H_2PO_4^-$.

Sensor	Solvent	Fluorophore	λ_{em} (nm)	Fluorescent mechanism	H : G stoichiometry	K_a determined from fluorescence	Ref.
1	CH_3CN	anthracene	415	PET	1 : 1	1.3×10^6 M^{-1}	28
2	CH_3CN : DMSO 9 : 1 (v/v)	anthracene	415	PET	1 : 1	$>1.3\times10^6$ M^{-1}	29
3	CH_3CN	anthracene	426	PET	1 : 1	1.6×10^5 M^{-1}	30
4	CH_3CN	anthracene	420	PET	1 : 1, 1 : 2	5.6×10^3 M^{-1}	32
5a	CH_3CN : DMSO : H_2O 98 : 1 : 1 (v/v/v)	benzthiazole	452	PET	1 : 1	7.9×10^3 M^{-1}	33
6	CH_3CN	isoquinolyl	395	PET	1 : 1	2.5×10^6 M^{-1}	34
7	CH_3CN	quinolyl	350	PET	1 : 1	2.8×10^6 M^{-1}	34
8	H_2O	naphthalene	478	displacement	1 : 1	1.8×10^6 M^{-1}	35
9	CH_3OH : HEPES buffer 1 : 1 (v/v)	2,2'-dihydroxyazobenzene	610	displacement	1 : 1	1.6×10^4 M^{-1}	36
10	CH_3OH	____	330	ligand-to-metal charge transfer	1 : 2	1.0×10^5 M^{-2}	37

was induced by other common anions (F^-, Cl^-, Br^-, I^-, AcO^-, HSO_4^-). Competitive experiments demonstrated that the presence of excess anions (50 equiv.) did not cause any significant changes in the emission of **3** with $H_2PO_4^-$ (5 equiv.).

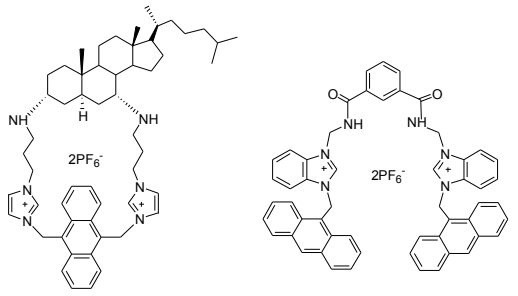

3 **4**

Fig. 2 Structures of sensors **3** and **4**.

Ghosh and co-workers have[32] designed and synthesised a flexible anthracene linked benzimidazolium-based receptor (**4**) (Fig. 2) which could be used as a "turn-off" fluorescent sensor for $H_2PO_4^-$ over other common anions. The fluorescence was quenched by 72% after addition of 2 equiv. of $H_2PO_4^-$ in CH_3CN, while no other changes such as excimer emission were observed. The binding constant was found to be 5.6×10^3 M^{-1}. A Stern-Volmer plot of sensor **4** with $H_2PO_4^-$ indicated both static and dynamic quenching effects. Since further addition of $H_2PO_4^-$ induced an increase in emission of sensor **4**, the authors suggested a two-step process of complexation: 1 : 1 binding occurred initially, and then changed to a 1 : 2 (host : guest) stoichiometry when in the presence of excess $H_2PO_4^-$.

A benzthiazole-based fluorescent sensor (**5a**) (Fig.3) was developed for the detection of $H_2PO_4^-$ by Lee and co-workers.[33] In order to evaluate its anion recognition performance, receptor **5b** was synthesised. The results showed that among all the tested common anions, only $H_2PO_4^-$ resulted in the significant fluorescence quenching of sensor **5a** in CH_3CN/DMSO/H_2O (98 : 1 : 1, v/v/v) with a binding constant of 7.9×10^3 M^{-1}, and no significant anion-binding interactions occurred with sensor **5b**. The high selectivity of sensor **5a** was attributed to the specific combination of both hydrogen bond-donating and -accepting moieties within the rigid cleft.

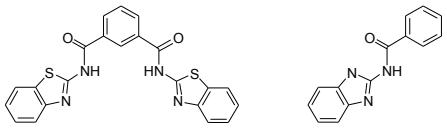

5a **5b**

Fig. 3 Structures of sensors **5a** and **5b**.

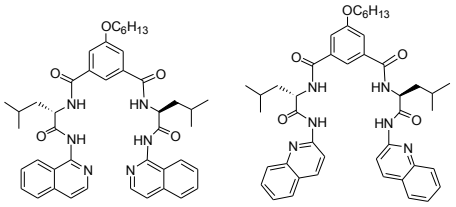

6 **7**

Fig. 4 Structures of sensors **6** and **7**.

Recently, Kondo et al.[34] reported selective detection of $H_2PO_4^-$ in CH_3CN utilizing the fluorescence quenching effect. The synthesised tetraamide-based sensors (**6** and **7**) contain isoquinolyl and quinolyl moieties respectively (Fig 4). Especially, sensor **7** bearing 2-quinolyl groups showed selective and nearly complete quenching by $H_2PO_4^-$, whereas it showed small or no changes towards other anions. The high selectivity of sensors **6** and **7** for $H_2PO_4^-$ (K_a = 2.5×10^6 M^{-1} and 2.8×10^6 M^{-1} respectively)

can be attributed to the additional hydrogen bonds formed between $H_2PO_4^-$ and the nitrogen atom of the isoquinolyl and quinolyl moieties.

2.2 "Displacement": releasing the non-fluorescent indicator

A pyrimidine-naphthalene anchored Schiff base (**8**) was synthesised by Kumar et al.[35] which was used as a "turn-on" fluorescent sensor for Al^{3+} in aqueous solution due to the inhibition of C=N isomerization after Al^{3+} complexation (Fig. 5). The formed **8**-Al^{3+} complex could also achieve the "turn-off" sensing of $H_2PO_4^-$ with a detection limit of 2.27×10^{-7} M via protonation of aldimine-nitrogen of sensor **8** by $H_2PO_4^-$. This releases the non-fluorescent **8** from the formed Al^{3+} complex. Unfortunately, HSO_4^- which has a lower pK_a value (1.99 vs. 3.88) also gave rise to the similar fluorescence quenching behaviour, while other common anions showed no fluorescent response.

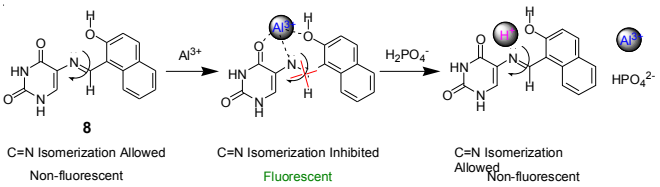

Fig. 5 Sensing mechanism of sensor **8** towards $H_2PO_4^-$.

The mononuclear 2,2'-dihydroxyazobenzene (DHAB)-Zn^{2+} complex (Fig. 6) was developed as a cost-effective "on-off" $H_2PO_4^-$ sensor based on the "displacement" protocol in CH_3OH/HEPES buffer (1 : 1, v/v).[36] Obvious fluorescence quenching of the Zn^{2+}-**9** complex, after addition of $H_2PO_4^-$ was observed due to $H_2PO_4^-$-induced decomposition of the DHAB-Zn(II) complex releasing the non-fluorescent DHAB. An opposite increase in fluorescence was induced by CN^-, while minimal or no changes were observed for other anions. The Zn^{2+}-**9** complex could also be used as a colorimetric receptor for $H_2PO_4^-$ due to the marked solution colour changes.

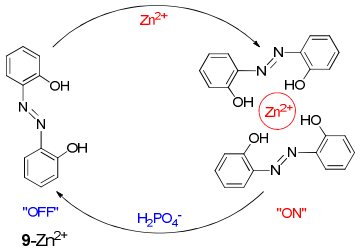

Fig. 6 Sensing mechanism of sensor **9** towards $H_2PO_4^-$.

2.3 Other mechanisms

Chen et al.[37] prepared a fluorescent tetranuclear pentacoordinated Zn(II) complex (**10**) based on a cresolic oxygen bridging ligand (**L**) shown in Fig. 7. The fluorescent properties of **10** were attributed to the chelation of **L** to the Zn^{2+} centers, which enhanced the rigidity of **L**. After addition of $H_2PO_4^-$ to a CH_3OH solution of sensor **10** remarkable fluorescence quenching was observed with a binding constant of 1.0×10^5 M^{-2} (1 : 2 binding mode). This may be a result partly from the electron repelling effect of $H_2PO_4^-$ and partly from the decrease of ligand rigidity because of $H_2PO_4^-$ binding. Both effects can prohibit the ligand-to-metal charge transfer reducing the fluorescence intensity. Other common anions only caused moderate fluorescence quenching or even enhancement of the fluorescence of sensor **10**.

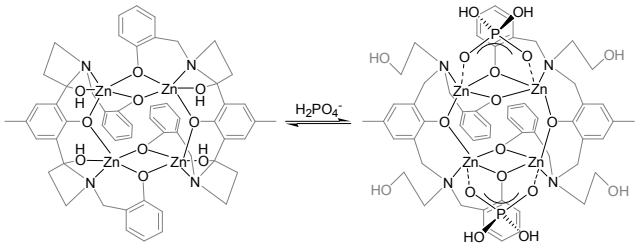

10

Fig. 7 Proposed binding mode of sensor **10** with $H_2PO_4^-$.

3. Intensity-based "turn-on" fluorescent sensors for $H_2PO_4^-$

In this section, the advances in "turn-on" $H_2PO_4^-$ fluorescent probes will be described. Compared with the "turn-off" type, these are preferable as they circumvent some of the drawbacks of fluorescence quenching, for example, the limited sensitivity and restricted practical applications. Fluorescence enhancement can occur by a number of pathways such as the prohibition of PET (Section 3.1 and Scheme 2b), the increase of rigidity of the sensors (Section 3.2) and "displacement" which releases the fluorescent indicator after addition of $H_2PO_4^-$ (Section 3.3). The spectroscopic and analytical parameters of each "turn on" fluorescent sensor for $H_2PO_4^-$ have been summarized in Table 2.

3.1 Inhibition of PET

A benzimidazolium-based macrocyclic fluorescent sensor (**11a**) (Fig. 8) was reported by Ghosh et al.[38] Significant fluorescence enhancement of sensor **11a** after binding $H_2PO_4^-$ was observed in CH_3CN which was assumed to be related to the deactivation of the PET process occurring between the macrocyclic binding domain and the excited state of the BINOL fluorophore. Furthermore, other anions, except fumarate, interacted weakly with sensor **11a**. The selectivity and binding affinity of sensor **11a** towards $H_2PO_4^-$ was greater than the acyclic sensor **11b** (K_a = 1.2×10^4 M^{-1} and 7.5×10^3 M^{-1} respectively).

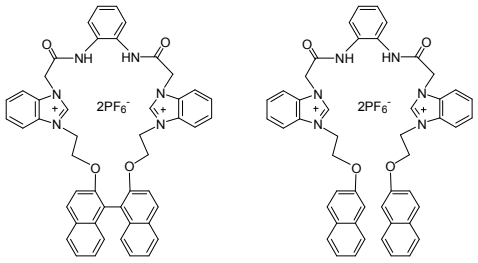

11a **11b**

Fig. 8 Structures of sensors **11a** and **11b**.

By inhibiting the PET process from an anthracene fluorophore to pyridinium moieties, Gong et al.[39] developed a $H_2PO_4^-$ fluorescent sensor (**12**) (Fig. 9). The sensor **12** displayed an excellent $H_2PO_4^-$ selectivity over the tested common anions in both $CHCl_3$ and CH_3CN by significant enhancement of monomer emission of anthracene. Interestingly, it was found that during the titration in $CHCl_3$, two-mode sensing of $H_2PO_4^-$ was exhibited: addition of less than equimolar $H_2PO_4^-$ induced the enhancement of excimer emission of the anthracene moiety alone, while

Table 2 Spectroscopic and analytical parameters of the "turn on" fluorescent sensors for $H_2PO_4^-$.

Sensor	Solvent	Fluorophore	λ_{em} (nm)	Fluorescent mechanism	H : G stoichiometry	K_a determined from fluorescence	Ref.
11a	CH_3CN	binaphthol	365	PET	1 : 1	1.2×10^4 M^{-1}	38
12	CH_3CN	anthracene	420	PET	1 : 1	____	39
13	CH_2Cl_2 : CH_3OH 9 : 1 (v/v)	anthracene	421	PET	1 : 1	2.8×10^3 M^{-1}	40
14	CH_3CN	anthracene	432	PET, rigidity effect	1 : 2	5.5×10^9 M^{-2}	41
15	DMSO	Schiff-base	333	PET, rigidity effect	1 : 1	____	42
16	CH_3CN	quinoline	393	PET, rigidity effect	1 : 1	3.3×10^4 M^{-1}	43
17	CH_3CN	Ru-complex	608	rigidity effect	1 : 2	7.6×10^9 M^{-2}	44
18	DMSO	binaphthol	396	rigidity effect	1 : 1	5.0×10^3 M^{-1}	45
19	CH_3CN : MOPS buffer 3 : 1, (v/v)	naphthalimide	540	displacement	____	____	46
20	CH_3CN	acridine	422	additional hydrogen bond	1 : 2	$>10^8$ M^{-2}	47
21	DMSO : HEPES buffer 1 : 9 (v/v)	Schiff-base	525	intramolecular hydrogen bond	1 : 1	2.0×10^3 M^{-1}	48

continuous addition until 3 equiv. of $H_2PO_4^-$ made significant enhancement of only monomer emission overwhelming the excimer emission. However, in the polar solvent CH_3CN, only the enhancement of monomer emission was observed during the whole titration. The possible binding process of sensor **12** with $H_2PO_4^-$ in $CHCl_3$ was proposed in Fig. 9.

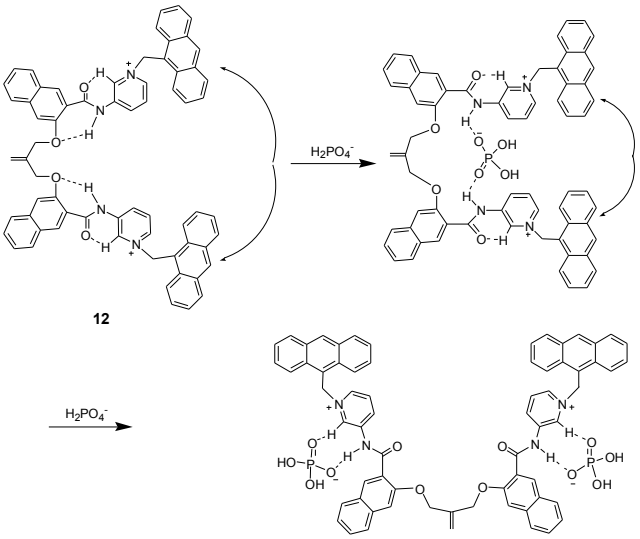

12

Fig. 9 Possible binding mode of sensor **12** with $H_2PO_4^-$ in $CHCl_3$.

Recently, Cao et al.[40] synthesised an anthracene-based fluorescent sensor (**13**) bearing two 1,2,3-triazolium groups (Fig. 10). The sensor **13** showed efficient fluorescence enhancement after addition of $H_2PO_4^-$ in CH_2Cl_2/CH_3OH (9 : 1, v/v) with a binding constant of 2.8×10^3 M^{-1}, while no obvious change was observed for other common anions. The presence of 100 equiv. of other anions did not cause any significant change for the emission of sensor **13** with 50 equiv. of $H_2PO_4^-$. The unique fluorescence enhancement of **13** induced by $H_2PO_4^-$ can be attributed to the formation of the $(C\text{-}H)^+\cdots O$ interaction which diminished acceptor properties of the triazolium ions inhibiting the PET process from anthracene to the charged triazoliums.

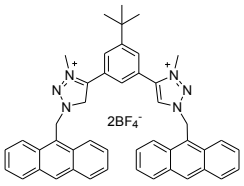

13

Fig. 10 The structure of sensors **13**.

A neutral fluorescent sensor (**14**) (Fig. 11) based on a calix[4]arene tetraamide derivative and anthracene was synthesised by Chen and co-workers.[41] The fluorescence of sensor **14** was efficiently enhanced about 130% $[(I\text{-}I_0)/I_0]$ upon addition of 5 equiv. of $H_2PO_4^-$ in CH_3CN. More importantly, it exhibited a high selectivity for $H_2PO_4^-$ over a wide range of common anions. The binding constant between **14** and $H_2PO_4^-$ was 5.5×10^9 M^{-2} with a 1 : 2 stoichiometry. The effective emission enhancement of sensor **14** towards $H_2PO_4^-$ is probably due to the inhibition of PET or the increased rigidity.

A simple $H_2PO_4^-$ fluorescent sensor (**15**) bearing phenol and thiourea binding sites was developed by Shao and co-workers.[42] The presence of $H_2PO_4^-$ induced the "off-on" fluorescence of **15** in DMSO. This is presumably due to both the inhibition of PET

and the binding-induced increased rigidity of the sensor. A distinct colour change was also observed, which could be attributed to the deprotonation of the phenol. The binding constant of **15** with $H_2PO_4^-$ was determined to be 5.6×10^4 M^{-1}. Unfortunately, F^- and AcO^- exhibited significant interference for the detection of $H_2PO_4^-$ using sensor **15**.

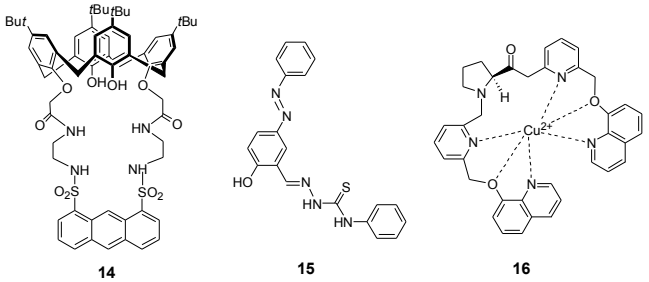

Fig. 11 Structures of sensors **14-16**.

Goswami et al.[43] developed a Cu^{2+}-based fluorescent sensor (**16**) for $H_2PO_4^-$ in CH_3CN. In the absence of $H_2PO_4^-$, the Cu^{2+}-complex was in a fluorescence-quenching state. However, when in the presence of $H_2PO_4^-$, the emission intensity of the complex increased dramatically, while much smaller increases in intensity were observed for other anions. The binding constant between **16** and $H_2PO_4^-$ was measured to be 3.3×10^4 M^{-1}. The metal complex might form a suitable cavity for the selective inclusion of $H_2PO_4^-$, as a consequence, the rigidity of the formed complex increased after $H_2PO_4^-$ complexation. In addition, the anion binding may also suppress the extent of electron transfer between the quinolines and Cu^{2+} resulting in the fluorescence enhancement.

3.2 Increase of rigidity effect

As mentioned for sensors **14-16**, apart from the inhibition of PET, the rigidity effect has been employed to explain the fluorescence enhancement upon anion binding. Indeed the increased rigidity of the formed binding complex could make the non-radiative decay from the excited state less probable and consequently, the emission intensity increases.[17]

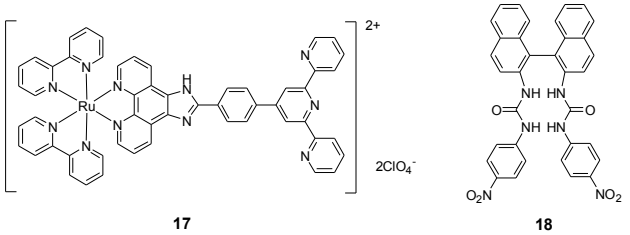

Fig. 12 Structures of sensors **17-18**.

Ruthenium(II) complex (**17**) (Fig. 12) has been developed as a selective fluorescent sensor for $H_2PO_4^-$ in CH_3CN.[44] Almost 3-fold fluorescence enhancement of sensor **17** was observed after addition of 10 equiv. of $H_2PO_4^-$. The enhanced emission of **17** in the presence of $H_2PO_4^-$ was caused by the formation of a hydrogen bond between $H_2PO_4^-$ and imidazolyl NH which increased its rigidity and planarity. The binding constant determined by fluorescence was as large as 7.6×10^9 M^{-2} (1 : 2 binding mode). In contrast, the same amount of F^- and AcO^- resulted in significant fluorescence quenching due to the deprotonation of NH, while the changes induced by other common anions were negligible. It is worth mentioning that sensor **17** can also be used as a colorimetric receptor for Fe^{2+} in CH_3CN/HEPES (1 : 71, v/v) and is thus a bifunctional sensor.

Huang et al.[45] designed and synthesised an easily prepared $H_2PO_4^-$ fluorescent sensor (**18**) containing urea group based on binaphthyl. The sensor **18** displayed switch-on fluorescence and the largest binding constant towards $H_2PO_4^-$ in DMSO. Upon complexation with $H_2PO_4^-$, sensor **18** was rigidified, causing the vibrational and rotational relaxation modes of non-radiative decay inhibited, leading to the increase of emission. Unfortunately, F^- and AcO^- can also give rise to the fluorescence enhancement with similar binding constants ($\sim10^3$ M^{-1}).

3.3 "Displacement": releasing the fluorescent indicator

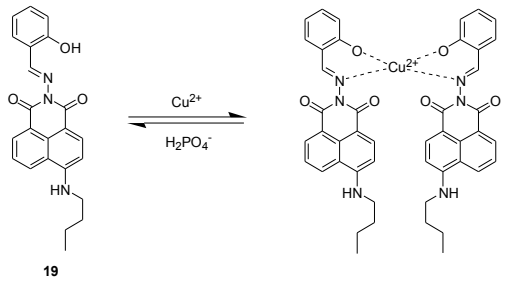

Fig. 13 Sensing mechanism of sensor **19** towards $H_2PO_4^-$.

A naphthalimide derivative (**19**) (Fig. 13) was developed as a fluorescent sensor by Chen and co-workers.[46] The sensor **19** displayed obvious fluorescence quenching in the presence of Cu^{2+} in CH_3CN/MOPS buffer (3 : 1 v/v) due to the inherent paramagnetic nature of Cu^{2+}. The formed metal complex exhibited a reversible fluorescence enhancement after addition of $H_2PO_4^-$, while the disturbances of other common anions were subtle. The retrievable "off-on" fluorescent behaviour of sensor **19** can be attributed to the release of the fluorescent **19** from the formed Cu^{2+}-**19** complex after addition of $H_2PO_4^-$.

3.4 Other mechanisms

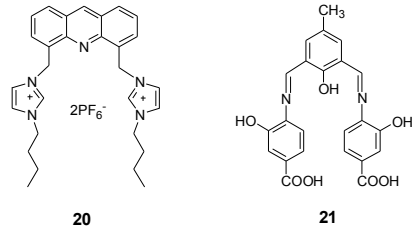

Fig. 14 Structures of sensors **20** and **21**.

An acridine derivative, bearing two imidazolium groups, as a selective fluorescent sensor (**20**) (Fig. 14) for $H_2PO_4^-$ has been developed by Kim and co-workers.[47] Significant increase of the fluorescence of **20** was observed after addition of $H_2PO_4^-$ in CH_3CN, while fluorescence quenching behaviour was observed for other anions. The binding constant of **20** with $H_2PO_4^-$ was measured to be larger than 10^8 M^{-2} with a 1 : 2 stoichiometry. Compared with their previously reported $H_2PO_4^-$ "turn-off" fluorescent sensor (**1** in Fig. 1), the only difference is the central nitrogen atom on the acridine fluorophore. Thus the authors inferred that the additional hydrogen bond formed between the nitrogen on the acridine moiety and $H_2PO_4^-$ afforded the anion-induced fluorescence enhancement.

Recently, a new fluorescent sensor (**21**) for $H_2PO_4^-$ based on a

Schiff-base was reported by Sen and co-workers.[48] After excitation in the visible region wavelength (480 nm), the sensor **21** could detect $H_2PO_4^-$ optically by the unique fluorescence enhancement at 525 nm in DMSO/HEPES buffer (1 : 9, v/v) with a detection limit of 3.5×10^{-6} M. The binding constant was determined to be 2.0×10^3 M^{-1}. The response was due to the formation of the intermolecular hydrogen bonds between $H_2PO_4^-$ and sensor breaking the intramolecular hydrogen bonding network between the three phenol residues. In addition, the presence of other common anions did not affect the detection of $H_2PO_4^-$. Bio-imaging studies indicated that sensor **21** is an efficient staining agent and could be used for monitoring intracellular $H_2PO_4^-$.

4. Ratiometric fluorescent sensors for $H_2PO_4^-$

Realizing ratiometric fluorescent sensing of $H_2PO_4^-$, which involves the ratio of fluorescence intensities at two different wavelengths before and after $H_2PO_4^-$ binding, is a current research focus. Compared with the "turn-off" or "turn-on" fluorescent sensors, ratiometric fluorescent probes present several advantages, for example they permit signal rationing and thus increase the dynamic range and provide built-in correction for environmental effects. In addition, the distinct fluorescent colour change after anion complexation will be practically useful for both visual sensing and convenient bio-imaging of anions. A typical mechanism affording this phenomenon is the formation or extinction of an intramolecular (Section 4.1, Scheme 3a and Table 3) or intermolecular (Section 4.2, Scheme 3b and Table 4) excimer. This will give rise to a change of the intensity ratio between monomer and excimer emissions of the fluorophore based upon the amount of the added anions. ESPT and other principles will also be described in Section 4.3 and 4.4 (Table 5).

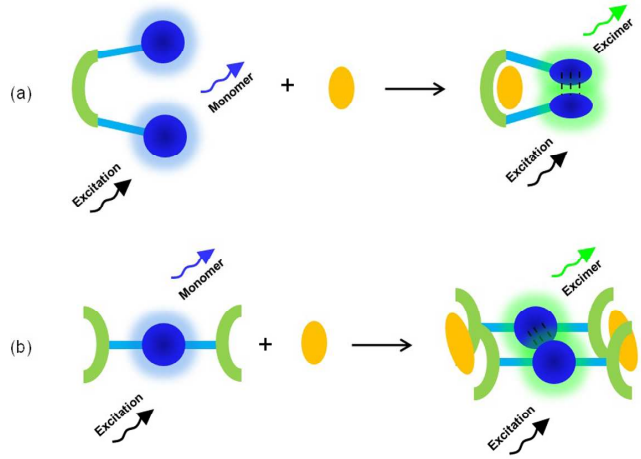

Scheme 3 Diagrams for (a) the intramolecular excimer formation and (b) the intermolecular excimer formation after anion binding.

4.1 Intramolecular excimer formation/extinction

A series of tweezer-like fluorescent sensors (**22-27**) (Fig. 15 and 16) have been developed by Ghosh and co-workers.[49-54] These sensors utilized an intramolecular excimer based on either naphthalene, anthracene or pyrene fluorophores. By incorporating benzimidazolium or amide moieties as anion binding sites, these sensors could achieve ratiometric sensing of $H_2PO_4^-$ either in organic or aqueous media with moderate binding constants ($\sim 10^4$ M^{-1}) but high sensing selectivity.

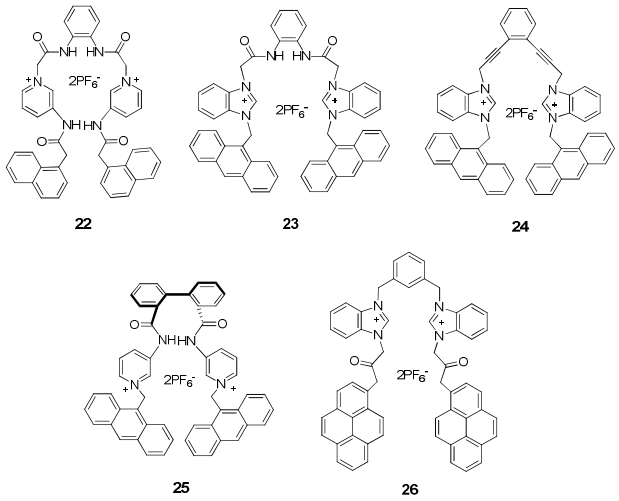

Fig. 15 Structures of sensors **22-26**.

The ortho-phenylenediamine based sensor **22**[49] could selectively bind $H_2PO_4^-$ in CH_3CN by exhibiting excimer emission at 456 nm due to the π-π stacking between two pendant naphthalene fluorophores. The sensor **23**,[50] based on the same ortho-phenylenediamine unit, could recognize $H_2PO_4^-$ in CH_3CN displaying a significant decrease of monomer emission of anthracene, along with a weak increase of excimer emission at 525 nm. A ratiometric change in emission after addition of $H_2PO_4^-$ was also achieved by the enediyne scaffold based sensor **24**[51] in CH_3CN containing 1% DMSO. Compared with **23**, in spite of the absence of the amide moieties as hydrogen bonding sites in sensor **24**, the binding constant of sensor **24** with $H_2PO_4^-$ was larger than that of **23** (5.4×10^3 vs. 3.1×10^4 M^{-1}) possibly because the linear nature of the triple bonds in **24** make the sensor more rigid. Pyridinium amide-based sensor **25**[52] built on a biphenyl scaffold showed selective complexation of $H_2PO_4^-$ with the enhancement of both monomer and excimer emission at 413 and 513 nm respectively in $CHCl_3$ containing 2% CH_3CN. By utilizing pyrene as the signalling unit, the benzimidazolium-based sensor **26**[53] was synthesised and used as an efficiently ratiometric fluorescent sensor for $H_2PO_4^-$ in CH_3CN due to its capacity of forming an excimer with pyrene.

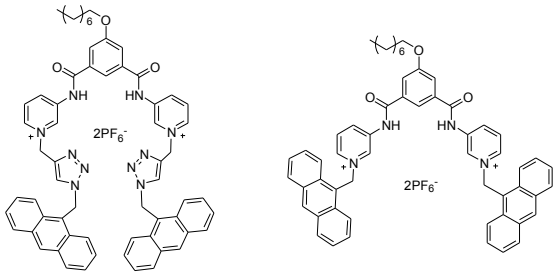

Fig. 16 Structures of sensors **27a** and **27b**.

An anthracene-labeled 1,2,3-triazole-linked bispyridinium sensor (**27a**)[54] (Fig. 16) was also developed as a ratiometric fluorescent sensor for $H_2PO_4^-$ over other common anions in

Table 3 Spectroscopic and analytical parameters of the ratiometric $H_2PO_4^-$ fluorescent sensors following the mechanism of intramolecular excimer.

Sensor	Solvent	Fluorophore	$\lambda_{monomer\ emission}$ (nm)	$\lambda_{excimer\ emission}$ (nm)	H : G stoichiometry	K_a determined from fluorescence	Ref.
22	CH_3CN	naphthalene	350	456	1 : 1	$9.1\times10^3\ M^{-1}$	49
23	CH_3CN	anthracene	419	525	1 : 1, 1 : 2	$5.4\times10^3\ M^{-1}$	50
24	CH_3CN : DMSO 99 : 1 (v/v)	anthracene	418	500	1 : 1	$3.1\times10^4\ M^{-1}$	51
25	$CHCl_3$: CH_3CN 98 : 2 (v/v)	anthracene	413	513	1 : 1, 1 : 2	$1.2\times10^4\ M^{-1}$	52
26	CH_3CN	pyrene	403	482	1 : 1	$2.2\times10^4\ M^{-1}$	53
27a	CH_3CN	anthracene	412	507	1 : 2	$2.5\times10^4\ M^{-1}$, $2.2\times10^4\ M^{-1}$	54
28	CH_3CN	anthracene	420	485	1 : 1	$2.2\times10^5\ M^{-1}$	55
29	CH_3CN	anthracene	418	500	1 : 1, 1 : 3	____	57
30	THF	pyrene	377	477	1 : 1	$1.9\times10^5\ M^{-1}$	58
31	THF	pyrene	375	477	1 : 2	____	59
32	CH_3CN	pyrene	380	483	1 : 1	____	60
33	CH_3CN : CH_2Cl_2 : H_2O 1000 : 1 : 5 (v/v/v)	pyrene	396	485	1 : 1	$1.0\times10^5\ M^{-1}$	61

CH_3CN. Job's plot analysis demonstrated a 1 : 2 stoichiometry between host and guest, and the binding constants were $2.5\times10^4\ M^{-1}$ and $2.2\times10^4\ M^{-1}$ for the successive complexation of the guest molecules. Additionally, the sensor **27a** could form a stable gel after addition of $H_2PO_4^-$ in $CHCl_3/CH_3CN$ (9 : 1, v/v), which also provided a convenient approach for visually sensing $H_2PO_4^-$. Interestingly, the control sensor **27b** without the triazole links failed to form the gel with $H_2PO_4^-$, highlighting the crucial role played by the triazole links on gel formation and $H_2PO_4^-$ recognition.

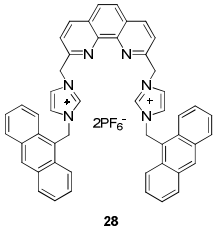

28

Fig. 17 The structure of sensor **28**.

Xu et al.[55] also developed a structurally similar ratiometric fluorescent sensor (**28**) (Fig. 17) for $H_2PO_4^-$ in CH_3CN based on imidazolium and anthracene groups. The sensor **28** displayed a unique excimer peak at 485 nm only in the presence of $H_2PO_4^-$ with a binding constant of $2.2\times10^5\ M^{-1}$. The addition of 10 equiv. of other anions did not cause any obvious change to the emission of **28** with $H_2PO_4^-$ (2 equiv.). The rigid phenanthroline moiety in sensor **28** allowed specific hydrogen bonds with $H_2PO_4^-$ accounting for the remarkable selectivity observed.

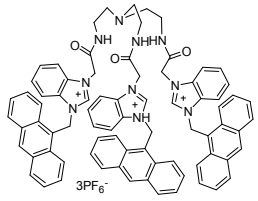

29

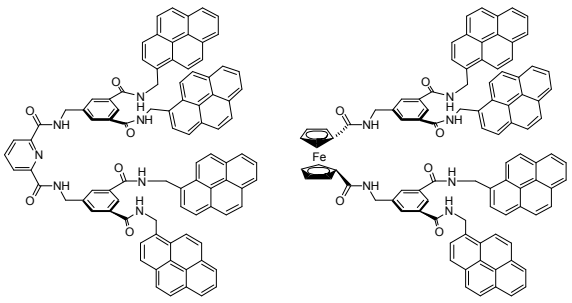

30 **31**

Fig. 18 Structures of sensors **29-31**.

Most $H_2PO_4^-$ ratiometric fluorescent sensors involving the formation of an intramolecular excimer contain two appended rigid fluorophores. However some sensors bearing multiple fluorophore substituents have been reported. It was believed that tripodal shaped receptors with anion binding groups attached on the three pendant arms would be able to complex anions effectively, due to their preferable pre-organization and conformational flexibility.[56] Thus Ghosh et al.[57] synthesised a

new benzimidazolium-based tripodal fluorescent sensor (**29**) (Fig. 18) bearing three pendant anthracene rings. The sensor **29** exhibited a high selectivity towards $H_2PO_4^-$ among all the common anions in CH_3CN via significant quenching of monomer emission (418 nm) along with the formation of a weak excimer at 500 nm.

A two-arm pyridine amide sensor (**30**) (Fig. 18) bearing four pyrenes as signal units was synthesised by Liao and co-workers.[58] This sensor, which provided a pseudo-tetrahedral cleft and multiple hydrogen bonds, formed a 1:1 complex with $H_2PO_4^-$ in THF leading to a significant decrease of the emission intensity ratio between the pyrene monomer (377 nm) and the excimer (477 nm). Further experiments demonstrated that the excimer emission of **30** was formed between two pyrene rings in different arms. Subsequently, a similar two-arm compound (**31**) based on ferrocene was developed as a ratiometric fluorescent sensor for $H_2PO_4^-$ by the same group.[59] The introduction of ferrocene offered another approach, i.e. cyclic voltammetry, for investigation of anion binding. Interestingly, in this case, the two-arm ferrocene hexamide sensor **31** formed a complex with $H_2PO_4^-$ with 1 : 2 stoichiometry: with each arm bound to one $H_2PO_4^-$ molecule independently. A synclinal conformation was adopted by sensor **31** in THF which was further stabilized by complexation with $H_2PO_4^-$.

The above-documented $H_2PO_4^-$ ratiometric sensors mostly relied on hydrogen bonding interactions. However, taking advantage of the ion-pairing electrostatic interaction between a metal ion and an anion, would also be useful as this would permit simultaneous binding of cationic and anionic species. It would also allow for a potential co-operative effect to be investigated, in which the anion/cation binding ability of the sensor could be significantly enhanced when in the presence of a bound cation/anion.

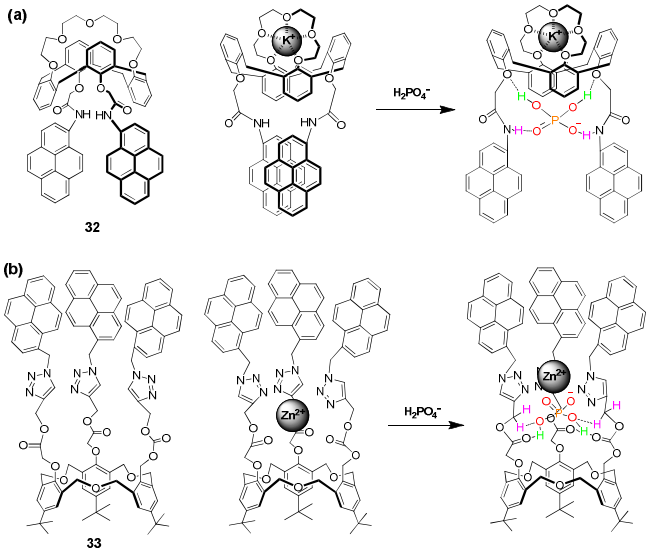

Fig. 19 Structures of sensors **32** and **33**, and their binding modes with metal ions and $H_2PO_4^-$.

A fluorescent sensor (**32**) (Fig. 19a) bearing pyreneamides as anion binding sites and a signalling unit based on calix[4]crown-5 has been designed and synthesised by Choi and co-workers.[60] The fluorescent excimer emission of **32** was first significantly increased after addition of K^+ in CH_3CN. Subsequently, it was observed that the excimer emission between the two pyrenes of **32**·K^+ declined obviously upon subsequent addition of $H_2PO_4^-$, while no change for other common anions occurred. The fact that the **32**·K^+ complex could achieve ratiometric sensing of $H_2PO_4^-$ while **32** cannot demonstrated that the binding of K^+ for **32** favoured the following association with $H_2PO_4^-$ as illustrated in Fig. 19a, i.e. the ion-pairing electrostatic interaction between K^+ and $H_2PO_4^-$ played an important role in the sensing behaviour. However, it cannot be neglected that to saturate sensor **32** a large excess of $H_2PO_4^-$ was required (10000 fold) and the K^+ coordinated complex might be decomposed at such high concentrations of $H_2PO_4^-$.

A Similar fluorescent sensor **33** (Fig. 19b) based on a pyrene-linked triazole-modified homooxacalix[3]arene was synthesised by Ni and co-workers.[61] The sensor showed ratiometric sensing of Zn^{2+} by enhancing the monomer emission while weakening the excimer in $CH_3CN/CH_2Cl_2/H_2O$ (1000 : 1 : 5, v/v/v). Interestingly, the subsequent addition of $H_2PO_4^-$ to the solution of **33**·Zn^{2+} resulted in a reversed ratiometric fluorescent change with a detection limit of 1.52×10^{-7} M. The binding constant was determined to be 1.0×10^5 M^{-1}. The observation that only small fluorescence intensity changes of monomer and excimer emissions of **33** were induced by $H_2PO_4^-$ indicated that **33**·Zn^{2+} played a key role in sensing of $H_2PO_4^-$. Furthermore, there is no interference for the detection of 40 equiv. of $H_2PO_4^-$ when in the presence of 40 equiv. of other anions.

4.2 Intermolecular excimer formation/extinction

Apart from intramolecular π-π stacking between two appended fluorophores, the intermolecular excimer which occurs between molecules is also a widely used strategy for designing ratiometric sensors. The change of the intensity ratio between the monomer and excimer emissions of the sensor when in the presence of a certain equivalent of anions in various concentrations can confirm whether the formation of excimer is intramolecular or intermolecular. If the values remain constant at different concentrations, the anion-induced excimer occurs intramolecularly. However if there is a change in the ratio, the excimer is being formed intermolecularly.[62]

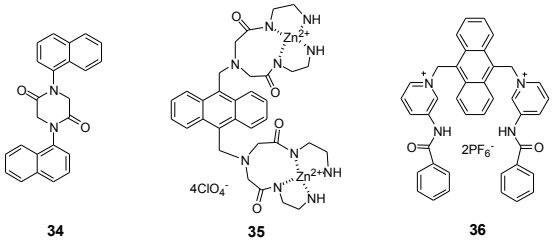

Fig. 20 Structures of sensors **34-36**.

A naphthalene-based 2,5-diketopiperazine (**34**) (Fig. 20) was developed as a ratiometric fluorescent sensor for $H_2PO_4^-$ in $CHCl_3$ containing 0.1% DMSO.[63] The monomer emission (338 nm) of sensor **34** was dramatically quenched when in the presence of $H_2PO_4^-$ along with the appearance of a weak excimer peak at 420 nm. The binding constant was measured to be 4.7×10^2 M^{-1} with UV method. The $H_2PO_4^-$-induced excimer was

Table 4 Spectroscopic and analytical parameters of the ratiometric $H_2PO_4^-$ fluorescent sensors following the mechanism of intermolecular excimer.

Sensor	Solvent	Fluorophore	$\lambda_{monomer\ emission}$ (nm)	$\lambda_{excimer\ emission}$ (nm)	H : G stoichiometry	K_a determined from fluorescence	Ref.
34	$CHCl_3$: DMSO 99.9 : 0.1 (v/v)	naphthalene	338	420	1 : 1	____	63
35	HEPES buffer	anthracene	432	490	1 : 1	$>4.6\times10^5$ M^{-1}	64
36	CH_3CN	anthracene	429	500	1 : 1	3.0×10^6 M^{-1}	65
37	CH_3CN	pyrene	400	493	1 : 1	2.4×10^6 M^{-1}	66
38a	CH_3CN	acridine	430	480	1 : 1	5.1×10^4 M^{-1}	67
39	CH_3CN	acridine	430	556	1 : 1	____	68
40	CH_3CN	acridine	430	544	1 : 1	____	68
41	CH_3CN	acridine	430	503	1 : 1	____	68
42	CH_3CN	acridine	430	466	1 : 1	____	68
43	CH_3CN	acridine	430	501	1 : 1	2.9×10^6 M^{-1}	69
44a	CH_3CN	anthracene	428	500	1 : 1	2.6×10^5 M^{-1}	69

assigned to be an intermolecular interaction, since the bifunctional hydrogen bonding donor sites in $H_2PO_4^-$ are able to bring two naphthalene residues into close proximity by forming hydrogen bonds with the oxygen atoms between two neighboring diketopiperazines. Unfortunately, aliphatic dicarboxylic acids, such as malonic, succinic, glutaric and adipic acids, could also give rise to the similar fluorescent behaviour, showing the poor selectivity of the sensor.

As metal-ligand receptors have a strong binding affinity for anions in competitive media, Huang et al.[64] synthesised an anthracene derivative (**35**) containing Zn^{2+} sites as a ratiometric fluorescent sensor for $H_2PO_4^-$. This sensor showed a selective fluorescence enhancement of the excimer emission at 490 nm as well as decrease of monomer emission at 432 nm with $H_2PO_4^-$ in 0.01 M HEPES buffer, pH = 7.4. The binding constant was measured to be larger than 4.6×10^5 M^{-1} by fluorescence. The formation of the anthracene dimer between two molecules induced by $H_2PO_4^-$ was attributed to binding of $H_2PO_4^-$ within the four zinc binding sites as well as due to a favorable π-π interaction between two flat hydrophobic anthracene rings. Other common anions except SO_4^{2-} only cause a minor fluctuation in monomer emission. In the case of SO_4^{2-}, a weak excimer emission could be induced when 10 equiv. were added.

A similar anthracene derivative (**36**) bearing amidopyridinium groups as anion binding sites was developed as a fluorescent sensor for $H_2PO_4^-$.[65] A concentration-dependent experiment showed that a new excimer peak was observed at high concentration of **36**, demonstrating that the sensor has a tendency to aggregate in solution. The anion sensing results revealed that among all the tested anions, only $H_2PO_4^-$ could induce the strong excimer emission of **36** in CH_3CN with a binding constant of 3.0×10^6 M^{-1}, which can be attributed to $H_2PO_4^-$-templated assembly of sensor molecules forming the anthracene excimer. The detection limit was determined to be 3.62×10^{-7} M.

Taking advantage of the strategy of anion-induced intermolecular π-π stacking, recently, in our group we also synthesised a series of acyclic and macrocyclic $H_2PO_4^-$ ratiometric fluorescent sensors bearing benzimidazolium and urea groups as binding sites built on pyrene, acridine or anthracene fluorophore.[66-69]

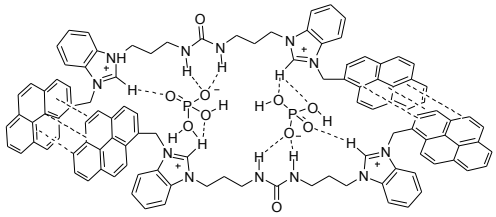

Fig. 21 The binding mode of sensor **37** with $H_2PO_4^-$.

Initially, the synthesis of a flexible pyrene-based fluorescent sensor **37** (Fig. 21) bearing benzimidazolium and urea groups was achieved.[66] This sensor was able to distinguish $H_2PO_4^-$ from other anions in CH_3CN by displaying ratiometric fluorescent sensing behaviour. Even though there are two pyrene rings per sensor molecule, the pyrene excimer was formed through an intermolecular pattern as illustrated in Fig. 21. This was demonstrated by the change of the intensity ratio of I_E/I_M which varied with the concentration of sensor **37** when in the presence of 2 equiv. of $H_2PO_4^-$. The detection limit of $H_2PO_4^-$ was achieved as 5.02×10^{-7} M. A synergistic effect between benzimidazolium and urea moieties can account for the high binding constant obtained ($K_a = 2.4\times10^6$ M^{-1}).

To investigate the synergistic binding effect more accurately, we further designed an acridine derivative (**38a**) containing benzimidazolium and urea moieties (Fig. 22).[67] For comparison, sensors **38b** and **38c** which only possess one type of binding site were prepared. Sensing results showed that **38a** could be used as a ratiometric fluorescent sensor for $H_2PO_4^-$ in CH_3CN by exhibiting a significant decrease of monomer emission at 430 nm and increase of the excimer at 480 nm with a binding constant of 5.1×10^4 M^{-1}. In contrast, the ratiometric sensing behaviours of sensors **38b** and **38c** toward $H_2PO_4^-$ were rather poor. A 2 : 2 binding complex was proposed between **38a** and $H_2PO_4^-$, which was directly detected by HRMS analysis. In addition, the sensor **38a** was also able to detect HSO_4^- in CH_3CN according to obvious fluorescence quenching ($K_a = 1.7\times10^6$ M^{-1}), while almost no response towards other anions was observed.

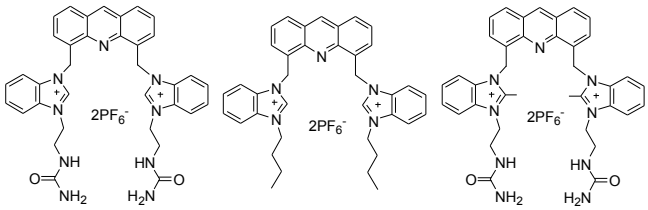

Fig. 22 Structures of sensors **38a-c**.

Macrocyclic anion receptors tend to display higher binding constants than their acyclic counterparts due to their well-preorganized topology. Therefore, we synthesised a series of acridine derived benzimidazolium macrocyclic sensors (**39-42**) (Fig. 23).[68] X-ray crystal structures revealed that these sensors had a tendency to aggregate forming acridine dimers. Anion binding studies showed that all the four sensors displayed "turn-on" as well as a bathochromic-shift in fluorescence emission only in the presence of $H_2PO_4^-$ in CH_3CN. Furthermore, different cavity size (**39**, **40** vs **41**) or rigidity (**40** vs **42**) of the sensors exhibited different bathochromic-shifts (from 36 to 126 nm) giving rise to various fluorescent colour changes. The tunable bathochromic-shifted emissions of these sensors induced by $H_2PO_4^-$ were attributed to anion-directed assembly of sensors forming the acridine excimers to a different extent.

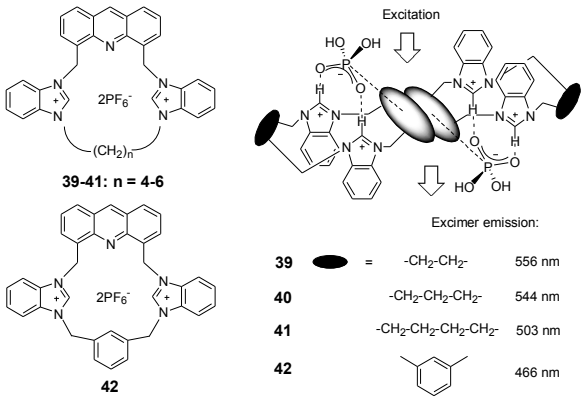

Fig. 23 Structures of sensors **39-42** and their binding modes with $H_2PO_4^-$.

In order to further improve the binding affinities of the macrocyclic sensors **39-42** with $H_2PO_4^-$, a urea moiety was then introduced. The aim being that the urea binding site would synergistically bind $H_2PO_4^-$ along with benzimidazolium moiety.[69] Results showed that compared with sensors **39-42**, the sensor **43** (Fig. 24) had a better ratiometric sensing performance toward $H_2PO_4^-$ in CH_3CN, such as a higher binding constant (2.9×10^6 M^{-1}) and lower detection limit (1.0×10^{-6} M). In addition, no significant variation in the intensity ratio (I_{501}/I_{430}) was found for the detection of 2 equiv. of $H_2PO_4^-$ when in the presence of 20 equiv. of other anions. Furthermore, interesting results were also achieved from a structurally similar anthracene cyclophane (**44a**) which exhibited an improved anion binding performance toward $H_2PO_4^-$ compared to the sensor **44b**, which incorporated only benzimidazolium groups (K_a = 2.6×10^5 M^{-1} and 1.6×10^5 M^{-1} respectively).

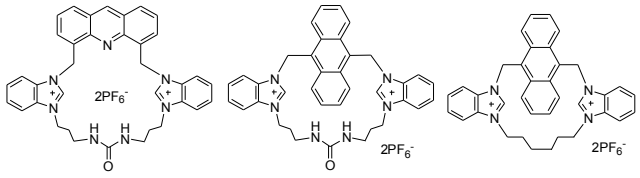

Fig. 24 Structures of sensors **43, 44a** and **44b**.

4.3 Intermolecular excited-state proton transfer

Excited-state proton transfer (ESPT) is an efficient approach utilized in the design of the ratiometric fluorescent sensors. The ESPT process generally incorporates a fast excited-state proton transfer from a proton donor (usually hydroxyl or amino group) to an acceptor group (often either oxygen or nitrogen) mediated by a hydrogen bond. In addition, a large apparent Stokes shift can be observed, which makes it very suitable for designing ratiometric fluorescent sensors. A specific illustration involving both PCT and ESPT can be seen in Scheme 4, apart from the emission channel from CT excited state, the proton transfer from the fluorophore to the anion can open the second emission channel, thus resulting in a ratiometric sensing behaviour. [70]

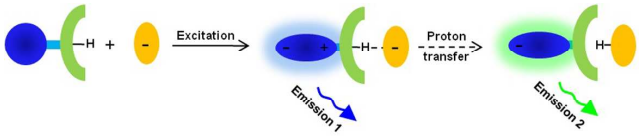

Scheme 4 The process of intermolecular excited state proton transfer between the receptor and anion.

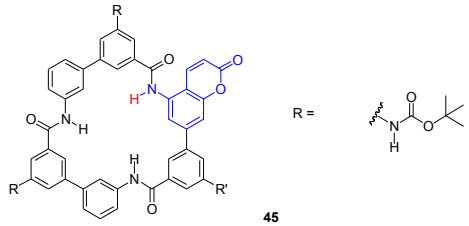

Fig. 25 The structure of sensor **45**.

With the strategy shown in Scheme 4, in 2001, Choi el al. reported the first ESPT-based ratiometric fluorescent sensor (**45**) (Fig. 25) built on the macrocyclic amide containing a coumarin fluorophore.[70] In DMSO/1,4-dioxane (1 : 1, v/v), the sensor **45** showed preferential binding towards tetrahedral anions,

Table 5 Spectroscopic and analytical parameters of the ratiometric $H_2PO_4^-$ fluorescent sensors following other mechanisms.

Sensor	Solvent	Fluorophore	Original λ_{em} (nm)	Induced λ_{em} (nm)	H : G stoichiometry	K_a determined from fluorescence	Ref.
45	DMSO : 1,4-dioxane 1 : 1 (v/v)	coumarin	430	540	1 : 1	2.0×10^6 M^{-1}	70
46	CH_3CN : H_2O 9 : 1 (v/v)	naphthalene	343	412	1 : 1	1.0×10^5 M^{-1}	74
47	$CHCl_3$	acridine	420	510	____	____	75
48	CH_3CN : DMSO 99.99 : 0.01 (v/v)	azaindole	365	480	1 : 1	2.0×10^4 M^{-1}	76
49	CH_3CN : DMSO 99.99 : 0.01 (v/v)	azaindole	365	480	1 : 1	1.1×10^4 M^{-1}	77
50	CH_3CH_2OH/THF 3 : 1 (v/v)	hexaphenylbenzene	438	366	____	____	78

especially for $H_2PO_4^-$ with a binding constant of 2.0×10^6 M^{-1}. In addition to a weak increase of the initial CT band at 430 nm after addition of $H_2PO_4^-$, a remarkable new emission band at 540 nm was observed. This was argued to be induced by proton transfer from the coumarin excited state to $H_2PO_4^-$. The intensity of the second emission band was related with the basicity of the anions tested. It should be noted that after this case, further examples using this mechanism have been reported for the detection of basic anions such as F^- and AcO^-.[71-73]

4.4 Other mechanisms

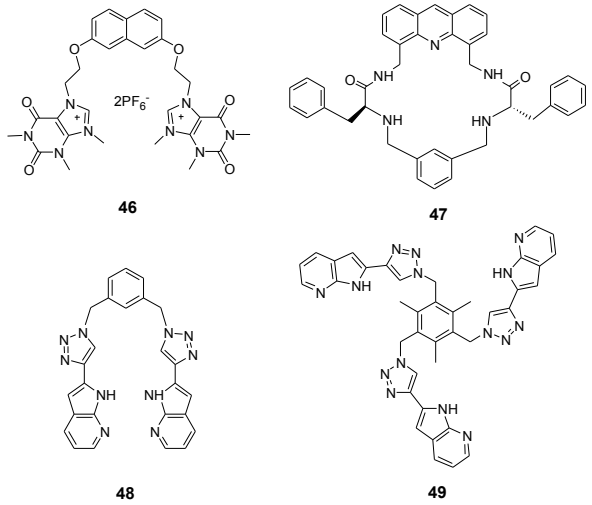

Fig. 26 Structures of sensors **46-49**.

The receptor **46** (Fig. 26) bearing theophyllinium as the key binding motif and a naphthalene moiety as the sensing unit was synthesised by Mahapatra and co-workers.[74] This sensor could selectively recognize $H_2PO_4^-$ in CH_3CN/H_2O (9 : 1, v/v) by exhibiting a significant decrease of emission at 343 nm and increase of a broad emission at 412 nm with a binding constant of 1.0×10^5 M^{-1}. The appearance of the new fluorescence band at longer wavelength (412 nm) might be attributed to the 'conformational restriction' after anion binding or the inhibition of PET via charge transfer between the excited state of naphthalene and theophyllium binding sites. For other common anions, the emission of **46** was decreased to a small extent.

Martí-Centelles et al.[75] synthesised a macrocyclic fluorescent sensor (**47**) based on acridine fluorophore. Upon addition of various acids in $CHCl_3$, there is an increase in emission at 510 nm while the original emission at 420 nm disappeared only in the case of H_3PO_4. The fluorescent recognition of H_3PO_4 via a bathochromic-shift was attributed to the supramolecular interactions between $H_2PO_4^-$ and the strongly fluorescent acridinium ion generated by the acid protonation of **47**. This assumption was supported by the fact that no change in fluorescence was observed when **47** was titrated with $H_2PO_4^-$ or TFA alone, but the fluorescence significantly increased when simultaneously adding both TFA and $H_2PO_4^-$.

Recently, Ghosh et al. developed two azaindole-1,2,3-triazole based ratiometric fluorescent sensors **48**[76] and **49**[77] for $H_2PO_4^-$ in CH_3CN containing 0.01% DMSO. Both of the two sensors selectively exhibited a decrease in emission at 365 nm and a weak increase at 480 nm upon $H_2PO_4^-$ binding. The binding constants of **48** and **49** with $H_2PO_4^-$ were determined to be 2.0×10^4 M^{-1} and 1.1×10^4 M^{-1} respectively. The fluorescence quenching at 365 nm was argued to be due to a reduction in the difference between the lowest energy singlet excited state ($n\pi^*$) and the ground singlet state after $H_2PO_4^-$ complexation. The appearance of the peak at 480 nm was attributed to the increase in conjugation between azaindoles and triazoles. In addition, the sensor **49** could be used as an efficient "turn-on" fluorescent sensor for Cl^- in the same solvent. Furthermore, for practical applications, the sensor **48** showed no selectivity towards ATP, ADP and AMP in CH_3CN containing 0.01% DMSO/H_2O (4 : 1, v/v), while **49** could selectively recognize ATP over ADP and AMP and was used for the bio-imaging of ATP in Hela cells.

Bhalla et al.[78] designed and synthesised a hexaphenylbenzene-based derivative (**50**) (Fig. 27). This sensor showed fluorescence enhancement at 438 nm in the presence of Zn^{2+} in ethanol/THF (3 : 1, v/v) due to the suppression of PET from the imino nitrogens to the hexaphenylbenzene scaffold. Additionally, the Zn^{2+} ensemble of compound **50** exhibited a selective fluorescent response towards $H_2PO_4^-$: the emission band at 438 nm was quenched and a new hypochromatic-shifted band at 366 nm appeared. The fluorescent phenomenon was attributed to the

weakening of the existing **50**-Zn^{2+} bonds due to the interaction of $H_2PO_4^-$ with Zn^{2+}. The detection limit was 10^{-8} M. In the case of other anions, no significant change in emission was observed except with AMP which induced the enhancement of emission along with a slight hypochromatic-shift from 438 to 431 nm.

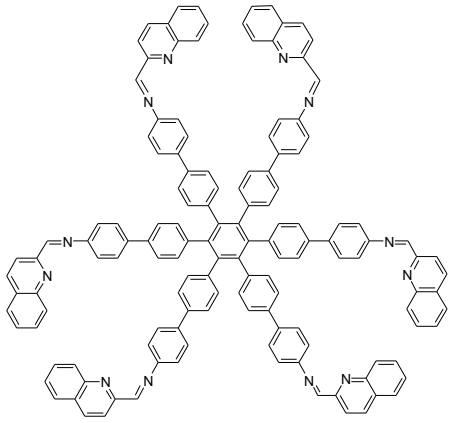

50

Fig. 27 The structure of sensor **50**.

5. Concluding remarks

In this review, $H_2PO_4^-$ fluorescent sensors based on synthetic organic molecules have been discussed. These sensors fluorescently detect $H_2PO_4^-$ utilizing either "turn-off", "turn-on" or ratiometric sensing behaviour. Promotion/inhibition of PET, binding-induced rigidity effect and intra/inter-molecular excimer formation/extinction are the most commonly employed principles involved in the process of $H_2PO_4^-$ recognition. Ratiometric fluorescent sensors utilizing the intra/inter-molecular excimer formed between fluorophores have been developed as the most successful strategy and are a current focus for future $H_2PO_4^-$ sensing.

Careful design of the binding site and structure has allowed the development of sensors that can selectively distinguish $H_2PO_4^-$. This can be achieved even in the presence of basic anions, such as F^- and AcO^-, and structurally similar tetrahedral anions such as HSO_4^-. However an even greater challenge, which still remains, is to selectively sense $H_2PO_4^-$ among inorganic/bio-phosphates such as $P_2O_7^{4-}$, ATP and ADP. In addition, most sensors utilize hydrogen bonding and so are only effective in organic solvents. Even though there are some metal complex based sensors that realize the recognition in water, the development of $H_2PO_4^-$ selective sensors for detection in aqueous media, is a major challenge for chemists. Furthermore, almost all of the reported sensors are only able to achieve qualitative detection of $H_2PO_4^-$ rather than quantitative determination. In spite of these deficiencies, science is advancing step by step, and so it can be expected that in the near future a relatively simple optical method for the selective, quantitative detection of the biologically important anion $H_2PO_4^-$ in aqueous solution will be available. This will be an important advance, as it may lead to a greater understanding of processes occurring within living cells and organs.

Acknowledgements

The authors are grateful to financial support from the National Natural Science Foundation of China (Grant No. 21072061) and Shanghai Leading Academic Discipline Project (Grant No. B409).

Notes and references

[a] *Shanghai Key Laboratory of Green Chemistry and Chemical Processes, Department of Chemistry, East China Normal University, 3663 North Zhongshan Road, Shanghai, 200062, P. R. China. Tel and Fax: +86(21)62233323, ghgao@chem.ecnu.edu.cn*

[b] *Laboratoire de Chimie, CNRS, École Normale Supérieure de Lyon, 46, Allée d'Italie, F-69364, Lyon, France. E-mail: alexandre.martinez@ens-lyon.fr*

† Electronic Supplementary Information (ESI) available: [details of any supplementary information available should be included here]. See DOI: 10.1039/b000000x/

‡ Footnotes should appear here. These might include comments relevant to but not central to the matter under discussion, limited experimental and spectral data, and crystallographic data.

1 W. Saenger, *Principles of Nucleic Acid Structure*, Springer, New York, 1998.
2 R. L. P. Adams, J. T. Knower, D. P. Leader, *The Biochemistry of Nucleic Acids, 10th ed.*, Chapman and Hall, New York , 1986.
3 P. A. Furman, J. A. Fyfe, M. H. St Clair, K. Weinhold, J. L. Rideout, G. A. Freeman, S. N. Lehrman, D. P. Bolognesi, S. Broder and H. Mitsuya, *Proc. Natl. Acad. Sci. U.S.A.*, 1986, **83**, 8333.
4 A. Ojida, Y. Mito-oka, K. Sada and I. Hamachi, *J. Am. Chem. Soc.*, 2004, **126**, 2454.
5 P. A. Gale, *Chem Commun.*, 2005, **30**, 3761.
6 A. E. Hargrove, S. Nieto, T. Zhang, J. L. Sessler and E. V. Anslyn, *Chem. Rev.*, 2011, **111**, 6603.
7 C. Bazzicalupi, A. Bencini and V. Lippolis, *Chem. Soc. Rev.*, 2010, **39**, 3709.
8 C. Warwick, A. Guerreiro and A. Soares, *Biosen. Bioelectron.*, 2013, **41**, 1.
9 T. Law al and S. B. Adeloju, *Talanta*, 2013, **114**, 191.
10 C. Spangler, M. Schaeferling and O. S. Wolfbeis, *Microchim. Acta*, 2008, **161**, 1.
11 M. Wenzel, J. R. Hiscock and P. A. Gale, *Chem. Soc. Rev.*, 2012, **41**, 480.
12 (a) A. Caballero, F. Zapata and P. D. Beer, *Coord. Chem. Rev.*, 2013. **257**, 2434. (b) H. T. Ngo, X. Liu and K. A. Jolliffe, *Chem. Soc. Rev.*, 2012, **41**, 4928.
13 L. Fabbrizzi and A. Poggi, *Chem. Soc. Rev.*, 2013, **42**, 1681.
14 (a) S. Kubik, *Chem. Soc. Rev.*, 2010, **39**, 3648. (b) S. J. Butler and D. Parker, *Chem. Soc. Rev.*, 2013, **42**, 1652.
15 B. M. Rambo, H. Y. Gong, M. Oh and J. L. Sessler, *Acc. Chem. Res.*, 2012, **45**, 1390.
16 T. Gunnlaugsson, M. Glynn, G. M. Tocci, P. E. Kruger and F. M. Pfeffer, *Coord. Chem. Rev.*, 2006, **250**, 3094.
17 R. Martínez-Máñez and F. Sancenón, *Chem. Rev.*, 2003, **103**, 4419.
18 J. S. Kim and D. T. Quang, *Chem. Rev.*, 2007, **107**, 3780.
19 R. M. Duke, E. B. Veale, F. M. Pfeffer, P. E. Kruger and T. Gunnlaugsson, *Chem. Soc. Rev.*, 2010, **39**, 3936.
20 X. Chen, X. Tian, I. Shin and J. Yoon, *Chem. Soc. Rev.*, 2011, **40**, 4783.
21 M. E. Moragues, R. Martínez-Máñez and F. Sancenón, *Chem. Soc. Rev.*, 2011, **40**, 2593.
22 J. Fan, M. Hu, P. Zhan and X. Peng, *Chem. Soc. Rev.*, 2013, **42**, 29.
23 Z. Xu, X. Chen, H. N. Kim and J. Yoon, *Chem. Soc. Rev.*, 2010, **39**, 127.
24 M. J. Culzoni, A. M. de la Peña, A. Machuca, H. C. Goicoechea and R. Babiano, *Anal. Methods*, 2013, **5**, 30.
25 P. de Silva, T. S. Moody and G. D. Wright, *Analyst*, 2009, **134,** 2385.
26 X. Qian, Y. Xiao, Y. Xu, X. Guo, J. Qian and W. Zhu, *Chem. Commun.*, 2010, **46**, 6418.
27 S. K. Kim, D. H. Lee, J. I. Hong and J. Yoon, *Acc. Chem. Res.*, 2008, **42**, 23.
28 S. K. Kim, N. J. Singh, S. J. Kim, H. G. Kim, J. K. Kim, J. W. Lee, K. S. Kim and J. Yoon, *Org. Lett.*, 2003, **5**, 2083.

29 J. Yoon, S. K. Kim, N. J. Singh, J. W. Lee, Y. J. Yang, K. Chellappan and K. S. Kim, *J. Org. Chem.*, 2004, **69**, 581.
30 J. R. Jadhav, C. H. Bae and H. S. Kim, *Tetrahedron Lett.*, 2011, **52**, 1623.
31 P. R. Brotherhood and A. P. Davis, *Chem. Soc. Rev.*, 2010, **39**, 3633.
32 K. Ghosh and D. Kar, *Beilstein J. Org. Chem.*, 2011, **7**, 254.
33 G. W. Lee, N. Singh, H. J. Jung and D. O. Jang, *Tetrahedron Lett.*, 2009, **50**, 807.
34 S. Kondo and R. Takai, *Org. Lett.*, 2013, **15**, 538.
35 A. Kumar, V. Kumar and K. K. Upadhyay, *Analyst*, 2013. **138**, 1891.
36 J. Wang and C. S. Ha, *Analyst*, 2010, **135**, 1214.
37 Z. Chen, X. Wang, J. Chen, X. Yang, Y. Li and Z. Guo, *New J. Chem.*, 2007, **31**, 357.
38 K. Ghosh and I. Saha, *Org. Biomol. Chem.*, 2012, **10**, 9383.
39 W. Gong, S. Bao, F. R. Wang, J. W. Ye, G. L. Ning and K. Hiratani, *Tetrahedron Lett.*, 2011, **52**, 630.
40 Q. Y. Cao, Z. C. Wang, M. Li and J. H. Liu, *Tetrahedron Lett.*, 2013. **54**, 3933.
41 Q. Y. Chen and C. F. Chen, *Eur. J. Org. Chem.*, 2005, 2468.
42 J. Shao, H. Lin and H. Lin, *Dyes Pigment*, 2009, **80**, 259.
43 S. Goswami, D. Sen and N. K. Das, *Tetrahedron Lett.*, 2010, **51**, 6707.
44 Z. B. Zheng, Z. M. Duan, Y. Y. Ma and K. Z. Wang, *Inorg. Chem.*, 2013, **52**, 2306.
45 W. Huang, H. Su, S. Yao, H. Lin, Z. Cai and H. Lin, *J. Fluoresc.*, 2011, **21**, 1697.
46 Z. Chen, L. Wang, G. Zou, X. Cao, Y. Wu and P. Hu, *Spectrochim. Acta. Part A*, 2013. 114, 323.
47 S. K. Kim, D. Seo, S. J. Han, G. Son, I. J. Lee, C. Lee, K. D. Lee and J. Yoon, *Tetrahedron*, 2008, **64**, 6402.
48 S. Sen, M. Mukherjee, K. Chakrabarty, I. Hauli, S. K. Mukhopadhyay and P. Chattopadhyay, *Org. Biomol. Chem.*, 2013, **11**, 1537.
49 K. Ghosh and I. Saha, *New J. Chem.*, 2011, **35**, 1397.
50 K. Ghosh, I. Saha and A. Patra, *Tetrahedron Lett.*, 2009, **50**, 2392.
51 K. Ghosh, S. S. Ali and S. Joardar, *Tetrahedron Lett.*, 2012, **53**, 2054.
52 K. Ghosh, A. R. Sarkar and A. Patra, *Tetrahedron Lett.*, 2009, **50**, 6557.
53 K. Ghosh, D. Kar and P. R. Chowdhury, *Tetrahedron Lett.*, 2011, **52**, 5098.
54 K. Ghosh, A. R. Sarkar and A. P. Chattopadhyay, *Eur. J. Org. Chem.*, 2012, 1311.
55 Z. Xu, S. Kim, K. H. Lee and J. Yoon, *Tetrahedron lett.*, 2007, **48**, 3797.
56 M. J. Berrocal, A. Cruz, I. H. A. Badr and L. G. Bachas, *Anal. Chem.*, 2000, **72**, 5295.
57 K. Ghosh and I. Saha, *Supramol. Chem.*, 2011, **23**, 518.
58 J. H. Liao, C. T. Chen and J. M. Fang, *Org. Lett.*, 2002, **4**, 561.
59 L. J. Kuo, J. H. Liao, C. T. Chen, C. H. Huang, C. S. Chen and J. M. Fang, *Org. Lett.*, 2003, **5**, 1821.
60 J. K. Choi, K. No, E. H. Lee, S. G. Kwon, K. W. Kim and J. S. Kim, *Supramol. Chem.*, 2007, **19**, 283.
61 X. L. Ni, X. Zeng, C. Redshaw and T. Yamato, *J. Org. Chem.*, 2011, **76**, 5696.
62 X. L. Wu, L. Luo, L. Lei, G. H. Liao, L. Z. Wu and C. H. Tung, *J. Org. Chem.*, 2008, **73**, 491.
63 K. Ghosh and T. Sen, *J. Incl. Phenom. Macrocycl. Chem.*, 2010, **68**, 447.
64 X. H. Huang, Y. B. He, C. G. Hu and Z. H. Chen, *Eur. J. Org. Chem.*, 2009, 1549.
65 W. Gong, Q. Zhang, F. Wang, B. Gao, Y. Lin and G. Ning, *Org. Biomol. Chem.*, 2012, **10**, 7578.
66 X. Jiang, D. Zhang, J. Zhang, J. Zhao, B. Wang, M. Feng, Z. Dong and G. Gao, *Anal. Methods*, 2013. **5**, 3222.
67 D. Zhang, X. Jiang, Z. Dong, H. Yang, A. Martinez and G. Gao, *Tetrahedron*, 2013, **69**, 10457.
68 D. Zhang, X. Jiang, H. Yang, A. Martinez, M. Feng, Z. Dong and G. Gao, *Org. Biomol. Chem.*, 2013, **11**, 3375.
69 D. Zhang, X. Jiang, H. Yang, Z. Su, E. Gao, A. Martinez and G. Gao, *Chem. Commun.*, 2013, **49**, 6149.
70 K. Choi and A. D. Hamilton, *Angew. Chem. Int. Ed.*, 2001, **40**, 3912.
71 B. Liu and H. Tian, *J. Mater. Chem.*, 2005, **15**, 2681.
72 X. Peng, Y. Wu, J. Fan, M. Tian and K. Han, *J. Org. Chem.*, 2005, **70**, 10524.
73 Y. Wu, X. Peng, J. Fan, S. Gao, M. Tian, J. Zhao and S. Sun, *J. Org. Chem.*, 2007, **72**, 62.
74 A. K. Mahapatra, G. Hazra and P. Sahoo, *Bioorg. Med. Chem. Lett.*, 2012, **22**, 1358.
75 V. Martí-Centelles, M. I. Burguete, F. Galindo, M. A. Izquierdo, D. K. Kumar, A. J. P. White, S. V. Luis and R. Vilar, *J. Org. Chem.*, 2011, **77**, 490.
76 K. Ghosh, D. Kar, S. Joardar, D. Sahu and B. Ganguly, *RSC Adv.*, 2013, **3**, 16144.
77 K. Ghosh, D. Kar, S. Joardar, A. Samadder and A. R. Khuda-Bukhsh, *RSC Adv.*, 2014, **4**, 11590.
78 V. Bhalla, V. Vij, M. Kumar, P. R. Sharma and T. Kaur, *Org. Lett.*, 2012, **14**, 1012.